

■ Porphyrinoids

β -to- β 2,5-Pyrrolylene-Linked Cyclic Porphyrin Oligomers

Yutao Rao,^[a] Jun Oh Kim,^[b] Woojae Kim,^[b] Guangming Zhong,^[a] Bangshao Yin,^[a] Mingbo Zhou,^[a] Hiroshi Shinokubo,^[c] Naoki Aratani,^[d] Takayuki Tanaka,^[e] Shubin Liu,^[f] Atsuhiko Osuka,^{*[e]} Dongho Kim,^{*[b]} and Jianxin Song^{*[a]}

Abstract: β -to- β 2,5-Pyrrolylene linked cyclic porphyrin oligomers have been synthesized by Suzuki–Miyaura coupling of 2,5-diborylpyrrole and 3,7-dibromoporphyrin. The cyclic porphyrin oligomers exhibit roughly coplanar structures, strong excitonic coupling, small electrochemical HOMO–LUMO gaps, and ultrafast excitation energy transfer between the neighboring porphyrins via the pyrrolylene bridge.

Cyclic porphyrin arrays have attracted wide attention owing to their potential applications, such as synthetic models of artificial photosynthetic antenna and large host molecules possessing convergent multidentate coordination sites.^[1–3] Cyclic porphyrin arrays are usually linked with acetylenic, aryl, heterocyclic, and other bridges. As rare and extreme cases, two spacerless directly meso-to-meso and β -to- β linked cyclic porphyrin arrays have been explored as photosynthetic models.^[4,5] These porphyrin nanorings display very efficient intramolecular exci-

tation energy transfer as a consequence of large electronic interaction of the constituent porphyrins. Pyrrole is a quite attractive bridge in cyclic porphyrin arrays in view of its electron-rich properties, significant conjugation with other segments, a potential hydrogen-bonding donor, and possible interconversion between amine-type and imine-type forms. Despite these promises, pyrrole-bridged porphyrin nanorings are rare. To the best of our knowledge, meso-to-meso pyrrole-bridged porphyrin nanorings were synthesized as a single example by Suzuki–Miyaura crossing coupling of 5,10-dibromoporphyrin and 2,5-diborylpyrrole.^[6] As an extension of this work, we report the synthesis of β -to- β 2,5-pyrrolylene-bridged cyclic porphyrin dimer and trimer (Figure 1).

3,7-Dibromo-10,15,20-triaryl Ni^{II} porphyrin **1Ni** was prepared by bromination of 3,7-diboryl-10,15,20-triaryl Ni^{II} porphyrin

[a] Y. Rao, G. Zhong, Dr. B. Yin, Dr. M. Zhou, Prof. Dr. J. Song
Key Laboratory of Chemical Biology and
Traditional Chinese Medicine Research (Ministry of Education of China)
Key Laboratory of Application and Assembly of
Organic Functional Molecules
Hunan Normal University, Changsha 410081 (China)
Fax: (+86) 731-8478-6676
E-mail: jxsong@hunnu.edu.cn

[b] J. O. Kim, W. Kim, Prof. Dr. D. Kim
Spectroscopy Laboratory for Functional π -Electronic Systems and
Department of Chemistry, Yonsei University
Seoul 03722 (Korea)
E-mail: dongho@yonsei.ac.kr

[c] Prof. Dr. H. Shinokubo
Department of Applied Chemistry, Graduate School of Engineering
Nagoya University, Nagoya 464-8603 (Japan)

[d] Prof. Dr. N. Aratani
Nara Institute of Science and Technology (Japan)

[e] Dr. T. Tanaka, Prof. Dr. A. Osuka
Department of Chemistry, Graduate School of Science
Kyoto University, Sakyo-ku, Kyoto 606-8502 (Japan)
Fax: (+81) 75-753-3970
E-mail: osuka@kuchem.kyoto-u.ac.jp

[f] Prof. Dr. S. Liu
Division of Research Computing, Information Technology Services
University of North Carolina, Chapel Hill, North Carolina 27599 (USA)

Supporting information and the ORCID identification number(s) for the author(s) of this article can be found under:
<http://dx.doi.org/10.1002/chem.201601306>

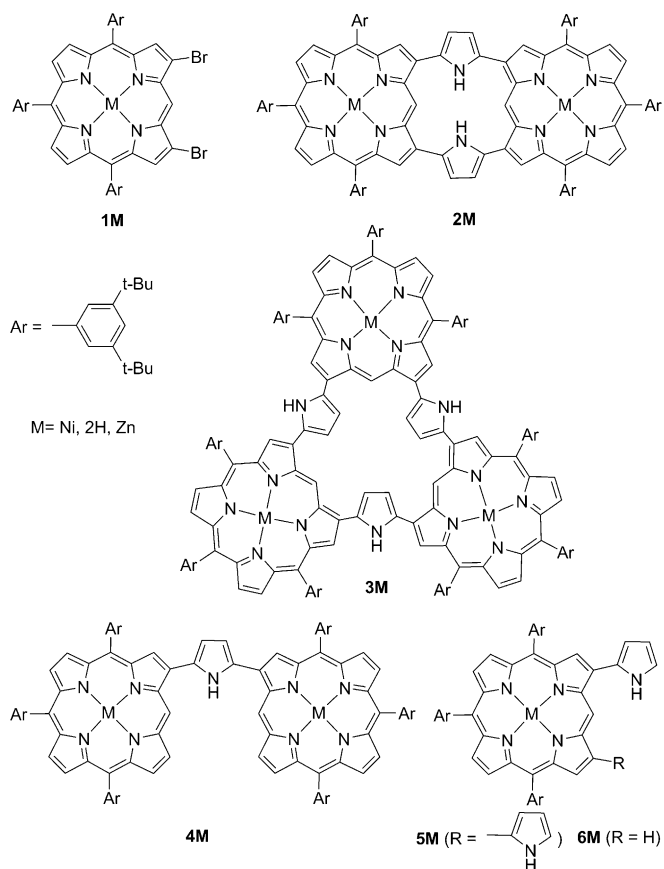


Figure 1. Porphyrin compounds studied herein.

with CuBr_2 in THF.^[5] Initially, Suzuki–Miyaura cross-coupling of **1Ni** and 2,5-diborylpyrrole^[7] was conducted under the same conditions used for meso-to-meso pyrrole-bridged porphyrin arrays ($\text{Pd}_2(\text{dba})_3$, PPh_3 , CsF , Cs_2CO_3 , DMF, toluene, reflux, 24 h).^[6] Mass analysis of the reaction mixture indicated formation of only linear oligomers and other unknown byproducts. Then we changed PPh_3 by $\text{P}(\text{tBu})_3$. To our delight, this reaction proceeded to give cyclic porphyrin dimer **2Ni** and trimer **3Ni** in 30% and 15% yields, respectively, after separation over a silica gel column. High-resolution electrospray-ionization time-of-flight (HR-ESI-TOF) mass measurement detected the parent ion peak of **2Ni** at $m/z = 1987.0353$ (calcd for $\text{C}_{132}\text{H}_{146}\text{N}_{10}\text{Ni}_2 = 1987.0439$ ($[\text{M}]^+$)), and that of **3Ni** at $m/z = 2981.5607$ (calcd for $\text{C}_{198}\text{H}_{219}\text{N}_{15}\text{Ni}_3 = 2981.5731$ ($[\text{M}]^+$)). The ^1H NMR spectra of **2Ni** and **3Ni** are both quite simple, exhibiting a set of signals for the porphyrins and bridges, indicating the molecular symmetry. The protons of the porphyrins were observed similarly for **2Ni** and **3Ni**, but the signals for the pyrrole bridges are remarkably different. The pyrrolic NH and β -protons are observed at $\delta = 10.36$ and 7.23 ppm for **2Ni** but the corresponding protons are observed at $\delta = 9.59$ and 7.96 ppm for **3Ni**. These chemical shifts differences may reflect different conformations of the pyrrole bridges, as shown in Figure 2.

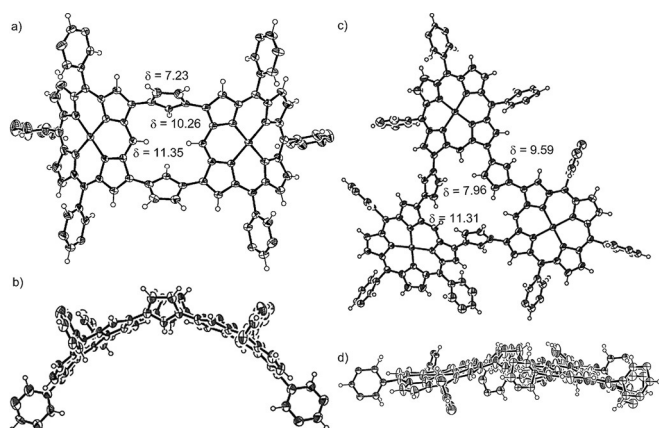


Figure 2. X-ray crystal structure of **2Ni** and **3Ni**. a) Top view and b) side view of **2Ni** and c) top view and d) side view of **3Ni**. Ellipsoids are set at 50% probability; substituents on phenyl groups and solvent molecules are omitted for clarity.

Definitive structural confirmations of **2Ni** and **3Ni** have been accomplished by X-ray diffraction analysis, which revealed diporphyrin and triporphyrin structures bridged by 2,5-pyrrolylene linkages (Figure 2).^[8] Dimer **2Ni** displays a rather bent gable structure with a diporphyrin dihedral angle of 111.6° , in which the pyrrole bridges are pointing inward. Trimer **3Ni** shows a more coplanar triangular molecular shape with the pyrrole bridges pointing outward. The structure of **3Ni** is distinctly more coplanar. The center-to-center distances are 10.72 Å for **2Ni** and 13.11 Å for **3Ni**, respectively.

In the next step, free-base porphyrin oligomers, **2H** and **3H**, and Zn^{II} porphyrin oligomers, **2Zn** and **3Zn**, were prepared.

Our attempts to demetallate **2Ni** and **3Ni** under acidic conditions failed. Dibromo free-base porphyrin **1H** was prepared by demetalation of dibromo Cu^{II} porphyrin **1Cu** and was used for the Suzuki–Miyaura coupling reaction with 2,5-diborylpyrrole to yield **2H** and **3H** in 20% and 9% yields, respectively. **2Zn** and **3Zn** were prepared almost quantitatively by Zn^{II} ion insertion of **2H** and **3H**. Singly 2,5-pyrrolylene-bridged dimers **4M** ($\text{M} = \text{Zn}, \text{Ni}, 2\text{H}$), 3,7-di(pyrro-2-yl)porphyrin monomers **5M** ($\text{M} = \text{Zn}, \text{Ni}, 2\text{H}$), and 2-(pyrro-2-yl)porphyrin monomers **6M** ($\text{M} = \text{Zn}, \text{Ni}, 2\text{H}$) were also synthesized by the same procedure as that of **2M** ($\text{M} = \text{Zn}, \text{Ni}, 2\text{H}$) for comparison of their spectroscopic properties.

Figure 3 shows the normalized UV/Vis absorption and fluorescence spectra of a series of Zn^{II} porphyrins measured in

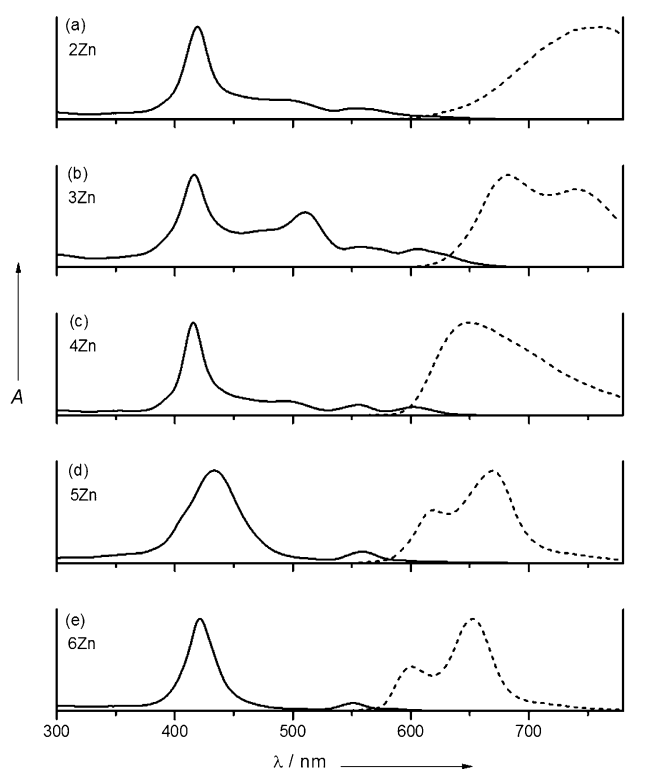


Figure 3. Normalized UV/Vis absorption (—) and fluorescence (-----) spectra of a) **2Zn**, b) **3Zn**, c) **4Zn**, d) **5Zn**, and e) **6Zn** in CH_2Cl_2 .

CH_2Cl_2 . Mono-pyrro-2-yl-substituted **6Zn** shows a Soret band at 420 nm and Q-band at 549 nm, both of which are slightly red-shifted compared to those of 5,10,15-triaryl Zn^{II} porphyrin (Soret band at 416 nm and Q-bands at 543 and 579 nm).^[9] The 0–0 band in the fluorescence spectrum of **6Zn** was observed at 605 nm with $\Phi_{\text{F}} = 0.027$, which is red-shifted and also very slightly enhanced as compared with that of the reference porphyrin ($\lambda_{\text{fl}} = 587$ nm and $\Phi_{\text{F}} = 0.023$). On the other hand, di(pyrro-2-yl)-substituted **5Zn** exhibits a more red-shifted and broader absorption spectrum with bands at 429 and 557 nm and fluorescence with $\lambda_{\text{fl}} = 618$ nm and $\Phi_{\text{F}} = 0.011$, which implies that two pyrrole units attached to adjacent β positions significantly affect the electronic structure of the porphyrin core.

β -to- β Pyrrolylene-bridged linear porphyrin dimer, **4Zn**, exhibits considerably enhanced 0–0 band intensity and relatively high fluorescence quantum yield compared to those of porphyrin monomers (Table 1). Dimer **4Zn** shows a large radiative rate constant, which is consistent with TD-DFT calculation that shows relatively high oscillator strength in the S_1 transition. Furthermore, the previous study on β -to- β directly linked porphyrin dimers, which reports its large fluorescence quantum yield and radiative rate constant owing to enhanced through-space MO interactions,^[10] is in good agreement with our observations on **4Zn**.

Table 1. Fluorescence quantum yields, fluorescence lifetimes, and radiative- and non-radiative rate constants of 2Zn–6Zn .				
Compound	$\Phi_{\text{fl}}^{[\text{a}]}$	$\tau_{\text{fl}}^{[\text{b}]}$ [ns]	$k_{\text{r}}^{[\text{c}]}$ [10^7 s^{-1}]	$k_{\text{nr}}^{[\text{c}]}$ [10^8 s^{-1}]
2Zn	0.002	1.4	0.14	7.1
3Zn	0.010	1.5	0.63	6.6
4Zn	0.065	1.7	3.8	5.5
5Zn	0.011	2.4	0.45	4.1
6Zn	0.027	2.4	1.1	4.0

[a] Absolute quantum yields for **2Zn–6Zn** are measured. [b] Fluorescence lifetimes are measured by time-correlated single photon counting technique in toluene solution. [c] Radiative and non-radiative rate constants are calculated on the basis of following equations: $\Phi_{\text{fl}} = k_{\text{r}} / (k_{\text{r}} + k_{\text{nr}})$ and $\tau_{\text{fl}} = 1 / (k_{\text{r}} + k_{\text{nr}})$.

Cyclic porphyrin oligomers **2Zn** and **3Zn** show distinctive spectral features in their absorption and fluorescence spectra. Cyclic dimer **2Zn** shows smeared long-tailing Q-band and a fluorescence peak around 755 nm with a large Stokes shift. Distinct excitonic coupling is evinced by a split Soret band ($\lambda_{\text{max}} = 419$ and 496 nm). Based on the TD-DFT calculations with the optimized geometry of **2Zn**, we found that the lowest excited state of **2Zn** is optically forbidden (Supporting Information, Figure S41), which accounted for its small fluorescence quantum yield (Table 1) and largely red-shifted fluorescence spectrum. Cyclic trimer **3Zn** also exhibits a split Soret ($\lambda_{\text{max}} = 416$ and 510 nm) and Q-bands ($\lambda_{\text{max}} = 557$ and 605 nm) with a relatively high extinction coefficient and enhanced Q(0,0) transition. These absorption data strongly suggest the large electronic interactions in **2Zn** and **3Zn**.

To investigate the electronic interaction between porphyrin units of **3Zn**, we first conducted fluorescence excitation anisotropy measurements, which enabled us to compare the relative orientation of the transition dipole moments between absorbing and emitting states. As shown in Figure S21, **3Zn** shows positive constant anisotropy values throughout the entire absorption spectrum. Given that both the rotational diffusion and excitation energy transfer (EET) processes are included at room temperature, this result indicates that the difference in angle between absorbing and emitting transition dipole moments is smaller than 54.7° where the fundamental anisotropy value is zero.^[11] In particular, and in contrast with the linear porphyrin oligomers, we observed that the anisotropy value at 420 nm, which corresponds to the Soret band of

monomeric moiety, obviously was positive, reflecting the arrangement of transition dipole moment within the triangular three porphyrin units.^[5b] The time-resolved fluorescence anisotropy measurements after photoexcitation at 420 nm clearly exhibit a positive initial anisotropy value in line with the excitation anisotropy result.

To get more detailed information on the EET processes occurring in **3Zn**, we have performed femtosecond transient absorption anisotropy (TAA) measurements. Pump wavelength was tuned to the lowest state of Q-band ($\lambda_{\text{pump}} = 610$ nm), which enabled us to exclude complicated processes arising from the upper excited states. Furthermore, multiple exciton generation was suppressed by using low pump-power conditions. As shown in Figure 4, fast depolarization process with

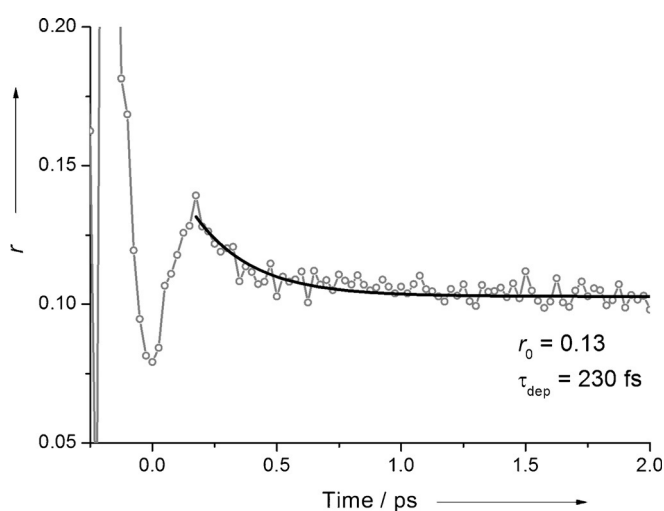


Figure 4. Transient absorption anisotropy (TAA) decay profiles of **3Zn** in toluene, where the pump and probe wavelengths are 610 nm and 520 nm, respectively.

a time constant of 230 fs was observed. This decay has been ascribed to energy transfer between the adjacent porphyrins. Based on the simple polygon model proposed by Fleming et al.,^[11] we could evaluate the excitation energy transfer time of cyclic **3Zn** as 690 fs. Importantly, this time constant of **3Zn** is approximately 200 times faster than the calculated rate of Förster-type resonance energy transfer (FRET; details are given in the Supporting Information). Since the FRET mechanism only depends on through-space energy transfer, the discrepancy between the experimentally observed and calculated EET rates indicates the importance of through-bond interaction via the pyrrole linkage. Furthermore, EET processes occurring in femtosecond time scale of **3Zn** indicates the strong electronic interactions between coplanar porphyrin moieties in the excited state. Interestingly, the EET time constant of **3Zn** is slightly slower than that of direct β -to- β linked cyclic porphyrin trimer (360 fs) but faster than that of 1,3-butadiyne bridged cyclic porphyrin trimer (1.4 ps).^[5] This comparison suggested that a 2,5-pyrrolylene bridge is effective in mediating the through-bond electronic interaction.

Table 2. Half-wave potentials of β -to- β pyrrolylene linked porphyrin arrays.^[a]

compound	$E_{\text{ox}1}$ [V] ^[b]	$E_{\text{red}1}$ [V] ^[b]	ΔE
2Ni	0.18	-1.91	2.09
3Ni	0.26	-1.48	1.74
4Ni	0.27	-1.83	2.10
5Ni	0.32	-1.82	2.14
6Ni	0.36	-1.81	2.17

[a] In dichloromethane with 0.1 M Bu_4PF_6 vs saturated calomel electrode (SCE). [b] Some potentials were determined by differential pulse voltammogram.

Finally, the electrochemical properties of **2Ni**, **3Ni**, **4Ni**, **5Ni**, and **6Ni** were investigated by cyclic voltammetry (Table 2). The cyclic voltammetry measurements of Ni^{II} porphyrins **2Ni**–**5Ni** were carried out in CH_2Cl_2 with 0.1 M Bu_4NPF_6 as supporting electrolyte (Supporting Information, Figure S27–S31). Monomers **5Ni** and **6Ni** display electrochemical HOMO–LUMO gaps that are typical of porphyrin monomers. In contrast, the cyclic oligomers **2Ni** and **3Ni** exhibit distinctly smaller HOMO–LUMO gaps, which is probably due to larger electronic interactions arising from the enforced cyclic structure. These HOMO–LUMO gaps are in good agreement with their optical HOMO–LUMO gaps.

In summary, β -to- β 2,5-pyrrolylene linked cyclic porphyrin dimer and trimer were synthesized by Suzuki–Miyaura coupling of 2,5-diborylpyrrole and 3,7-dibromoporphyrin. The cyclic porphyrin oligomers exhibit roughly coplanar structures, strong excitonic coupling, and small electrochemical HOMO–LUMO gaps. The cyclic trimer **3Zn** displays the ultrafast excitation energy transfer mediated by through-bond mechanism via the pyrrole linkage. Further extension of this coupling strategy to synthesize more elaborated porphyrin arrays is ongoing in our laboratories.

Acknowledgements

We thank Prof. Xiaoyi Yi (Central South University, China) for **3Ni** crystal measurement. The work at Hunan Normal University was supported by the National Natural Science Foundation of China (Grant No. 21272065), the Scientific Research Foundation for the Returned Overseas Chinese Scholars, State Education Ministry, and Scientific Research Fund of Hunan Provincial Education Department (Grant No. 13k027). The work at Kyoto was supported by a Grant-in-Aid from MEXT (No. 25220802 (Scientific Research (S))). The research at Yonsei University was supported by the Global Research Laboratory (GRL) Program (2013K1A1A2A02050183) of the Ministry of Education, Science and Technology (MEST) of Korea. The quantum calculations

were performed using the supercomputing resource of the Korea Institute of Science and Technology Information (KISTI).

Keywords: excitation energy transfer · exciton coupling · porphyrinoids · porphyrins · nickel

- [1] a) S. Anderson, H. L. Anderson, J. K. M. Sanders, *Acc. Chem. Res.* **1993**, *26*, 469; b) D. Holten, D. F. Bocian, J. S. Lindsey, *Acc. Chem. Res.* **2002**, *35*, 57; c) Y. Nakamura, N. Aratani, A. Osuka, *Chem. Soc. Rev.* **2007**, *36*, 831; d) N. Aratani, D. Kim, A. Osuka, *Acc. Chem. Res.* **2009**, *42*, 1922.
- [2] a) K. Sugiura, Y. Fujimoto, Y. Sakata, *Chem. Commun.* **2000**, 1105; b) A. Kato, K. Sugiura, H. Miyasaka, H. Tanaka, T. Kawai, M. Sugimoto, M. Yamashita, *Chem. Lett.* **2004**, *33*, 578; c) O. Shoji, H. Tanaka, T. Kawai, Y. Kobuke, *J. Am. Chem. Soc.* **2005**, *127*, 8598; d) J. E. Raymond, A. Bhaskar, T. D. Goodson III, N. Makiuchi, K. Ogawa, Y. Kobuke, *J. Am. Chem. Soc.* **2008**, *130*, 17212.
- [3] a) M. Hoffmann, C. J. Wilson, B. Odell, H. L. Anderson, *Angew. Chem. Int. Ed.* **2007**, *46*, 3122; *Angew. Chem.* **2007**, *119*, 3183; b) M. Hoffmann, J. Kärnbratt, M.-H. Chang, L. M. Herz, B. Albinsson, H. L. Anderson, *Angew. Chem. Int. Ed.* **2008**, *47*, 4993; *Angew. Chem.* **2008**, *120*, 5071; c) J. K. Sprafke, D. V. Kondratuk, M. Wykes, A. L. Thompson, M. Hoffmann, R. Drevinskas, W. H. Chen, C. K. Yong, J. Kärnbratt, J. E. Bullock, M. Malfois, M. R. Wasielewski, B. Albinsson, L. M. Herz, D. Zigmantas, D. Beljonne, H. L. Anderson, *J. Am. Chem. Soc.* **2011**, *133*, 17262; d) M. C. O'Sullivan, J. K. Sprafke, D. V. Kondratuk, C. Rinfray, T. D. W. Claridge, A. Saywell, M. O. Blunt, J. N. O'Shea, P. H. Beton, M. Malfois, H. L. Anderson, *Nature* **2011**, *469*, 72.
- [4] Y. Nakamura, I.-W. Hwang, N. Aratani, T. K. Ahn, D. M. Ko, A. Takagi, T. Kawai, T. Matsumoto, D. Kim, A. Osuka, *J. Am. Chem. Soc.* **2005**, *127*, 236.
- [5] a) H. Cai, K. Fujimoto, J. M. Lim, C. Wang, W. Huang, Y. Tao, S. Zhang, H. Shi, B. Yin, B. Chen, M. Ma, J. Song, D. Kim, A. Osuka, *Angew. Chem. Int. Ed.* **2014**, *53*, 11088; *Angew. Chem.* **2014**, *126*, 11268; b) S. Lee, H. Chung, S. Tokuji, H. Yorimitsu, A. Osuka, D. Kim, *Chem. Commun.* **2014**, *50*, 2947.
- [6] J. Song, N. Aratani, H. Shinokubo, A. Osuka, *Chem. Eur. J.* **2010**, *16*, 13320.
- [7] J. Takagi, K. Sato, J. F. Hartwig, T. Ishiyama, N. Miyaura, *Tetrahedron Lett.* **2002**, *43*, 5649.
- [8] Crystal data for **2Ni**: $\text{C}_{172.5}\text{H}_{146}\text{N}_{10}\text{Ni}_2\text{O}_9$, $M_w = 2620.41$, monoclinic, space group $P2_1/c$, $a = 15.6397(17)$ Å, $b = 27.818(3)$ Å, $c = 37.340(4)$ Å, $\beta = 92.791(2)^\circ$, $V = 16226(3)$ Å³, $Z = 4$, $D_{\text{calc}} = 1.073$ g cm⁻³, $T = 90(2)$ K, 83639 measured reflections, 28474 unique reflections, $R = 0.0945$, $R_w = 0.2846$ (all data), $\text{GOF} = 1.076$ ($I > 2.0\sigma(I)$). Crystal data for **3Ni**: $\text{C}_{172.5}\text{H}_{146}\text{N}_{10}\text{Ni}_2$, $M_w = 2985.01$, rhombohedral, space group $R\bar{3}$, $a = 29.2971(12)$ Å, $b = 29.2971(12)$ Å, $c = 44.137(2)$ Å, $V = 32808(3)$ Å³, $Z = 6$, $D_{\text{calc}} = 0.906$ g cm⁻³, $T = 90(2)$ K, 47021 measured reflections, 16569 unique reflections, $R = 0.0883$, $R_w = 0.2453$ (all data), $\text{GOF} = 1.02$ ($I > 2.0\sigma(I)$). CCDC 976093 (**2Ni**) and 976099 (**3Ni**) contain the supplementary crystallographic data for this paper. These data can be obtained free of charge from The Cambridge Crystallographic Data Centre.
- [9] K. Fujimoto, H. Yorimitsu, A. Osuka, *Chem. Eur. J.* **2015**, *21*, 11311.
- [10] S. Cho, M.-C. Yoon, J. M. Lim, P. Kim, N. Aratani, Y. Nakamura, T. Ikeda, A. Osuka, D. Kim, *J. Phys. Chem. B* **2009**, *113*, 10619.
- [11] S. E. Bradforth, R. Jimenez, F. van Mourik, R. van Grondelle, G. R. Fleming, *J. Phys. Chem.* **1995**, *99*, 16179.

Received: March 18, 2016

Revised: April 12, 2016

Published online on May 17, 2016